JACS
JOURNAL OF THE AMERICAN CHEMICAL SOCIETY

pubs.acs.org/JACS

Article

Facile H/D Exchange at (Hetero)Aromatic Hydrocarbons Catalyzed by a Stable Trans-Dihydride N-Heterocyclic Carbene (NHC) Iron Complex

Subhash Garhwal, Alexander Kaushansky, Natalia Fridman, Linda J. W. Shimon, and Graham de Ruiter*

Cite This: J. Am. Chem. Soc. 2020, 142, 17131−17139

Read Online

ACCESS | Metrics & More | Article Recommendations | Supporting Information

ABSTRACT: Earth-abundant metal pincer complexes have played an important role in homogeneous catalysis during the last ten years. Yet, despite intense research efforts, the synthesis of iron $PC_{carbene}P$ pincer complexes has so far remained elusive. Here we report the synthesis of the first $PC_{NHC}P$ functionalized iron complex $[(PC_{NHC}P)FeCl_2]$ (**1**) and the reactivity of the corresponding *trans*-dihydride iron(II) dinitrogen complex $[(PC_{NHC}P)Fe(H)_2N_2)]$ (**2**). Complex **2** is stable under an atmosphere of N_2 and is highly active for hydrogen isotope exchange at (hetero)aromatic hydrocarbons under mild conditions (50 °C, N_2). With benzene-d_6 as the deuterium source, easily reducible functional groups such as esters and amides are well tolerated, contributing to the overall wide substrate scope (e.g., halides, ethers, and amines). DFT studies suggest a complex assisted σ-bond metathesis pathway for $C(sp^2)$−H bond activation, which is further discussed in this study.

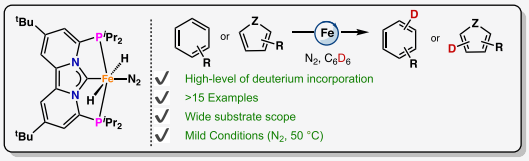

INTRODUCTION

Driven by their pre-eminent two-electron chemistry, the predictable reactivity and selectivity of precious metals have made them the premier choice as catalysts in many synthetic processes.[1] The growing environmental, economic, and geopolitical concerns associated with using precious metals, in conjunction with their limited availability, are strong incentives to rethink current strategies and establish more environmentally friendly alternatives.[2] One such methodology relies on using earth-abundant metals such as cobalt,[3] manganese[4] and in particular iron,[5] as catalyst for a variety of organic transformations.[6] Indeed, during the past decade we have seen a resurgence of using earth-abundant metals in homogeneous catalysis. One of the main reasons behind this resurgence is our ability to utilize the unique properties of earth-abundant metals (e.g., spin-state reactivity) via elaborate ligand designs.[7]

From the wide variety of available ligand architectures, pincer-type ligands have contributed tremendously to the development of earth-abundant metal catalysis.[8] The most commonly encountered structural motifs within this set of ligands are those featuring an XNX (X = NR, PR_2, $P(OR)_2$) pincer type geometry with a central amino or pyridine donor.[8] In contrast, earth-abundant metal pincer complexes presenting a carbene as central donor are virtually absent from the literature,[9] in particular those containing a $PC_{NHC}P$ type geometry (Figure 1).[10] Their absence is quite surprising as carbenes often impart distinct electronic and steric properties to the metal center.[11] For instance, when comparing PCP versus PNP pincer complexes of the second and third row transition metals, the PCP complexes featuring a central N-heterocyclic carbene (NHC) typically bind stronger to the metal center,[12] while simultaneously increasing its electron density,[13] which benefits catalyst stability and reactivity.[12a]

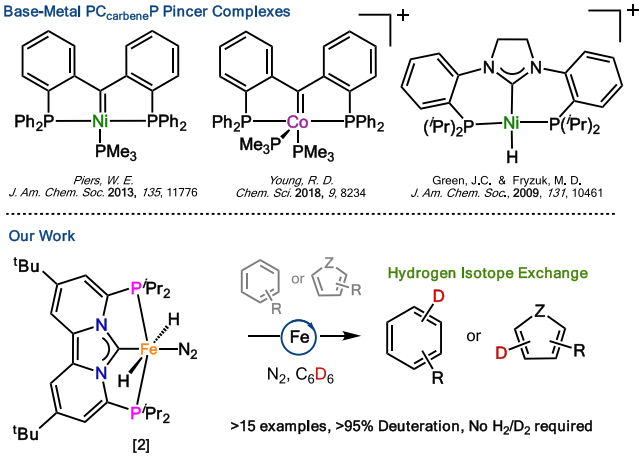

Figure 1. Selected examples of first-row transition-metal $PC_{carbene}P$ pincer complexes and the herein reported reactivity of $[(PC_{NHC}P)Fe(H)_2N_2)]$ (**2**).

Received: July 16, 2020
Published: September 9, 2020

https://dx.doi.org/10.1021/jacs.0c07689
J. Am. Chem. Soc. 2020, 142, 17131−17139

Yet, despite these advantages no catalytic activity of iron, cobalt, or manganese $PC_{NHC}P$ pincer complexes have been reported,[14] while synthetic methodologies to access these complexes for iron are currently lacking.[10b] Considering these limitations, developing NHC-centered phosphine-functionalized pincer complexes could hold great benefits for iron-based catalysis, especially when containing metal-hydrides.[15]

Here we report the synthesis and characterization of novel $PC_{NHC}P$ pincer complex $[(PC_{NHC}P)FeCl_2)]$ (**1**) that upon exposure to 2.2 equiv of $NaBHEt_3$ generates the first example of a stable *trans*-dihydride iron(II) dinitrogen complex $[(PC_{NHC}P)Fe(H)_2N_2)]$ (Scheme 1; **2**). Iron complex **2** is highly stable at room temperature and does not readily reductively eliminate H_2 upon exposure to N_2, which is a commonly observed deactivation pathway for other *trans*-dihydride iron(II) complexes lacking π-acidic CO ligands.[15b,16] The equatorial N_2 ligand in **2** is readily displaced under catalytic conditions enabling hydrogen/deuterium (H/D) exchange at (hetero)aromatic hydrocarbons with benzene-d_6 as deuterium source. Generally, the reaction occurs under mild conditions (N_2, 50 °C), and is tolerant of a variety of functional groups including, ethers, esters, amides, halides, and heterocycles. To the best of our knowledge, complex **2** is one of the very few iron-based catalysts capable of catalytic H/D exchange at heteroaromatics using a readily available deuterium source.

Scheme 1. Synthesis of $PC_{NHC}P$ Iron Complexes 1 and 2 and the Observed H/D Exchange in Benzene-d_6

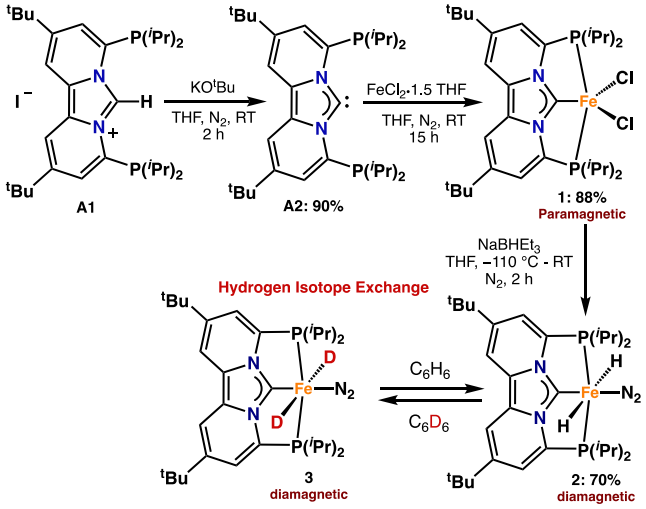

RESULTS AND DISCUSSION

Synthesis of Iron $PC_{NHC}P$ Pincer Complexes. Realizing the lack of current synthetic methodologies for preparing earth-abundant metal $PC_{NHC}P$ pincer complexes, we became interested in a ligand platform known as dipyrido[1,2-c;2′,1′-e]imidazolin-6-ylidenes,[17] whose rigid framework might allow for strong binding of earth-abundant metals. We commenced our studies by synthesizing azolium salt **A1** via a modification of a known literature procedure.[17a] Subsequent deprotonation of **A1** with potassium *tert*-butoxide (KO^{t}Bu) in THF resulted in the formation of free carbene **A2** (Scheme 1).

Addition of $FeCl_2$·1.5THF (1.1 equiv) to a stirred solution of **A2** in THF (15 mL) resulted in the formation of a new paramagnetic species (**1**) as judged by ^{1}H NMR spectroscopy (Figure S12). High-resolution mass spectrometry (HRMS) is consistent with the assignment of **1** as $[(PC_{NHC}P)FeCl_2)]$ (Figure S13), which was also confirmed by X-ray crystallography.

The solid-state structure of **1** is shown in Figure 2, and features an iron metal center in a distorted trigonal bipyramidal geometry. The axial phosphine donors are only weakly bound to the iron metal center, which is evident from the long iron phosphine distances of 2.782(2) Å (Fe−P1) and 2.765(2) Å (Fe−P2). The iron carbene (Fe−C1) distance of 2.062(6) and the NCN angle of 102.3(5)° are typical for other iron NHC complexes that are reported in the literature.[18]

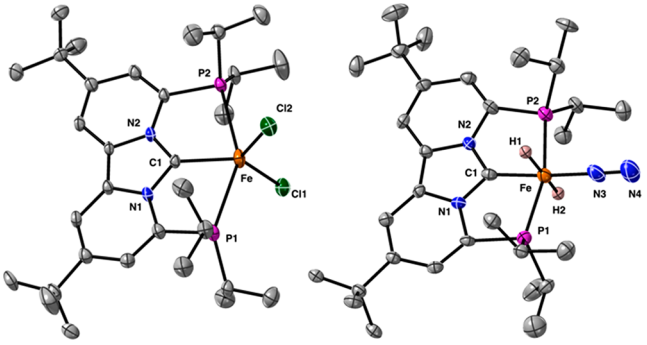

Figure 2. Solid state structures of $[(PC_{NHC}P)FeCl_2]$ (**1**, left) and $[(PC_{NHC}P)Fe(H)_2N_2]$ (**2**, right). Thermal ellipsoids are shown at the 30% probability level. Hydrogen atoms (except H1 and H2) and cocrystallized solvent molecules are omitted for clarity.

With iron $PC_{NHC}P$ pincer complex **1** in hand, we investigated its reactivity toward a variety of hydride donors, because of the wide applicability of transition-metal hydrides in catalysis.[8b,19] Addition, of two equiv of $NaBHEt_3$ to a THF solution of complex **1** at −110 °C afforded a new diamagnetic species (**2**) that is stable for several days in solution at room temperature (Scheme 1). The ^{1}H NMR spectrum of complex **2** exhibits a single characteristic triplet at −8.79 ppm (2H), whose $^2J_{P-H}$ values of 43.0 Hz are consistent with a tentative assignment of **2** as the *trans*-dihydride iron complex $[(PC_{NHC}P)Fe(H_2)N_2)]$. Additional T_1 measurements (at 298 K) support such a *trans*-dihydride assignment where the decay time of 420 ms is similar to those reported for other transition-metal *trans*-dihydride complexes.[15b,16] Definite structural assignment of **2** was provided by X-ray crystallography (Figure 2). Although the crystals were not of sufficient quality to allow comparison of the bond metrics, it does allow for identification of complex **2** as $[(PC_{NHC}P)Fe(H)_2N_2)]$ with the coordinated N_2 opposite to the $PC_{NHC}P$ carbene, forcing the two hydrides in a trans geometry. As a result, the combined spectroscopic (NMR) and crystallographic data confirm the formation of a stable classical iron(II) *trans*-dihydride, which is unprecedented.[20]

Hydrogen Isotope Exchange (HIE) at (Hetero)-Aromatics. The ability to selectively exchange hydrogen for either deuterium or tritium is important for understanding many fundamental processes in organometallic,[21] medicinal,[22] and biological chemistry.[23] Classically, HIE is catalyzed by noble metals such as ruthenium,[24] rhodium,[25] and iridium.[26] In contrast, only a few studies report on the HIE with earth-abundant metals.[27] Given the importance of earth-abundant metal-hydride species in hydrogen isotope exchange (HIE) reactions,[28] we reasoned that iron complex **2** could be a

https://dx.doi.org/10.1021/jacs.0c07689
J. Am. Chem. Soc. 2020, 142, 17131−17139

Table 1. Substrate Scope for Hydrogen Isotope Exchange at (Hetero)Aromatic Hydrocarbons, Catalyzed by 2[a,b]

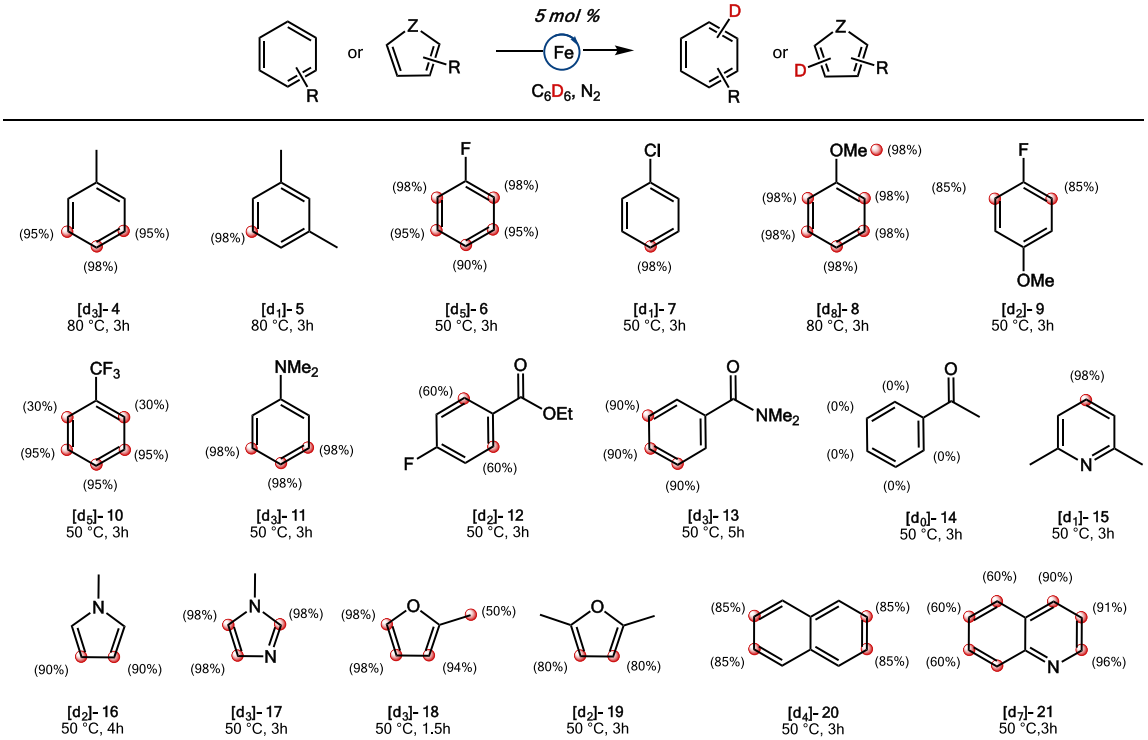

[a]See the Supporting Information for experimental details. [b]Yields were determined by ^{1}H NMR spectroscopy in the presence of an internal standard (tetraethylsilane).

straightforward entry toward facile H/D exchange at aromatic hydrocarbons.

Our studies into H/D exchange started with the observation that the hydride resonance at −8.79 ppm (t, $^2J_{P-H}$ = 43.0 Hz) in complex **2** slowly disappeared after dissolving **2** in benzene-d_6. No other changes in the ^{1}H NMR spectrum of **2** were observed. Analysis of the solution by ^{2}H and ^{31}P NMR spectroscopy revealed the appearance of a triplet (^{2}H) at −8.68 ppm ($^2J_{P-D}$ = 6.6 Hz) and a quintet (^{31}P) at 133.27 ppm ($^2J_{D-P}$ = 6.2 Hz), which is consistent with the formation of the dideuteride iron(II) complex **3** (Figure S3) Similarly, dissolving **3** in benzene results to the reformation of complex **2** in quantitative yields.

The reversible H/D exchange between the solvent and complex **2** indicates reversible C(sp^2)−H activation, which is promising for allowing catalytic HIE with other hydrocarbons.[25b,29] As evident from Table 1, complex **2** indeed efficiently catalyzes the H/D exchange between the solvent (benzene-d_6) and a variety of (hetero)aromatic hydrocarbons. The reaction occurs under mild conditions (N_2, 50−80 °C) and typically requires less than 3 h for high levels of deuterium incorporation. For example, toluene is exclusively deuterated at the meta and para positions (>95%), which are the sterically most accessible positions. (Table 1; [**d**$_3$]-**4**). Likewise, for *m*-xylene, the meta-position was preferentially deuterated (98%). In both substrates, deuteration of the ortho position was not observed. These data suggest that for toluene and *m*-xylene, the observed regioselectivity is primarily dictated by steric factors. Computational studies (vide infra) corroborated these findings and showed that for toluene C−H bond activation at the meta and para positions is energetically more favorable than at the ortho position (Table 2). Note, however, that by using elevated temperatures and longer reaction times different

Table 2. Relative Energies (ΔG) in kcal mol^{-1} of the Transition State (TS1-R) for C−H Exchange at the ortho, meta, and para Positions of Toluene, Fluorobenzene, Anisole, and Dimethylaniline[a,b]

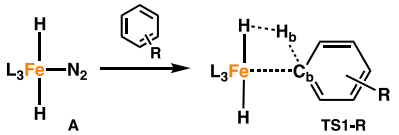

	position		
substituent	ortho	meta	para
R = H	25.2	25.2	25.2
R = Me	30.4	25.9	25.2
R = NMe_2	31.3	25.2	27.5
R = OMe	25.6	24.5	25.7
R = F	23.9	23.6	25.1

[a]Energies are reported relative to structure **A** (Figure 3). [b]See the Supporting Information for computational details.

regioselectivities can be observed (Figure S20 and S21). Notwithstanding, these results are akin to those obtained by Chirik[27f] and Leitner,[24a] whose iron and ruthenium pincer complexes; [H_4-^{iPr}CNC)Fe(N_2)$_2$] and [(PNP)Ru(H)$_2$(H_2)] showed comparable regioselectivity.

Encouraged by these initial results, we sought to increase the substrate scope to include a variety of electronically and sterically differentiated substrates (Table 1). For example, fluorobenzene was completely deuterated within 3 h (Table 1, [**d**$_5$]-**6**). Monitoring the reaction by ^{1}H and ^{19}F NMR spectroscopy revealed that the ortho and meta position are preferentially deuterated (Figure S71 and S72). Only after 30 min deuteration of the para position is observed, while

https://dx.doi.org/10.1021/jacs.0c07689
J. Am. Chem. Soc. 2020, 142, 17131−17139

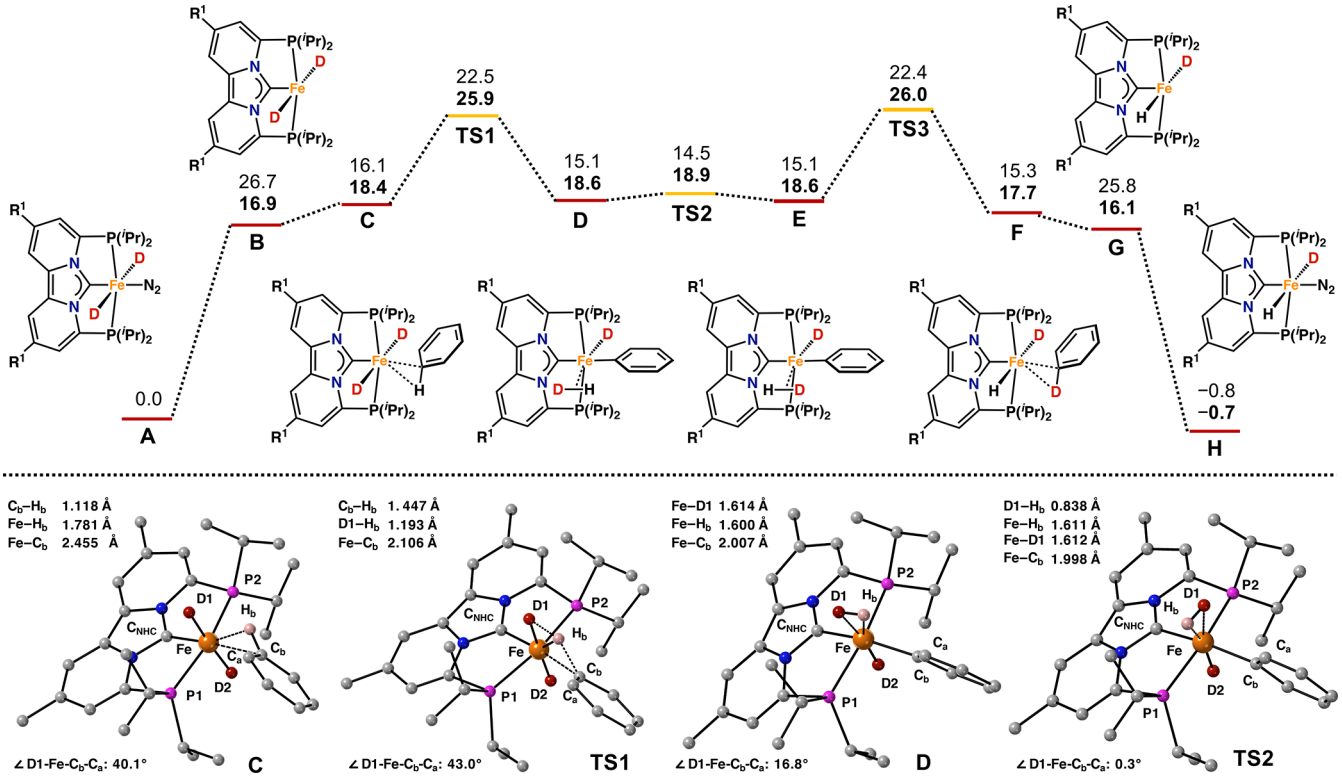

Figure 3. Calculated free energy profiles ($\Delta H/\Delta G$) in kcal mol^{-1} and plausible mechanistic pathways for hydrogen isotope exchange (HIE) of **3** with benzene. Hydrogen atoms (except H_b) are omitted for clarity. For computational details, see the Supporting Information.

complete deuteration of the para positions takes nearly 3 h. These results reflect the level of deuteration in the order of ortho (98%) > meta (95%) > para (90%) as shown in Table 1. Interestingly, for the related chlorobenzene deuterium incorporation was only observed at the para position, whereas for 4-fluoroanisole incorporation was observed at the ortho position (Table 1; [d_1]-**7** and [d_2]-**9**). Clearly, besides the established steric effects, electronic effects are important contributors to the observed regioselectivity (vide infra). More detailed computational studies regarding the observed regioselectivity and mechanism for H/D exchange are presented in Figure 3 and Table 2, and are further discussed in the computational section of this manuscript. Nonetheless, the ability of **2** to efficiently deuterate chlorobenzene demonstrates that the complex **2** is stable toward reductive elimination of H_2 and subsequent oxidative addition of the aryl halide.

Besides aryl halides, arenes bearing other electron withdrawing substituents were efficiently deuterated as well, albeit primarily at sterically accessible C(sp^2)−H bonds (Table 1; [$\mathbf{d_5}$]-**10**). In a similar manner, electron rich arenes were also efficiently deuterated. Dimethylaniline showed near quantitative incorporation of deuterium (>98%) at the meta and para positions, whereas for anisole complete deuteration was observed to yield anisole-d_8 within the course of 3 h (Table 1).

Substrates containing reducible substituents such as esters ([$\mathbf{d_2}$]-**12**) and amides ([$\mathbf{d_3}$]-**13**) are tolerated as well. For instance, ethyl 4-fluorobenzoate is selectively deuterated at the ortho position (60%), while *N*,*N*-dimethylbenzamide is selectively deuterated at the meta and para positions (Table 1). The difference in regioselectivity between [$\mathbf{d_2}$]-**12** and [$\mathbf{d_3}$]-**13** is due to different steric requirements of the directing group, although electronic effects from the fluorine atom cannot be excluded. Unfortunately, substrates containing ketones (e.g., acetophenone, benzophenone, and/or cyclohexyl phenyl ketone) are not susceptible for catalytic H/D exchange. It is known that iron-dihydride complexes are good ketone hydrogenation catalysts.[30] In the absence of a suitable proton donor, the iron-hydride is nucleophilic enough to attack the ketone to generate an alkoxide intermediate,[31] that is incapable of performing HIE. However, catalyst decomposition to form inactive Fe(I) or Fe(0) species cannot be excluded.[32] Nonetheless, these results do not negate the fact that complex **2**, tolerates several functional groups (e.g., halides, ethers, esters, amides, and/or heterocycles).

In addition to the various substituted aromatic hydrocarbons, heteroaromatic compounds are also good substrates for HIE.. For instance, in 5-membered heterocyclic compounds, such as *N*-methyl-pyrrole, 1-methylimidazole, 2-methylfuran, and 2,5-dimethylfuran, most aromatic protons were deuterated with incorporation levels ranging from 80 to 98% (Table 1, [$\mathbf{d_2}$]-**16**−[$\mathbf{d_2}$]-**19**). In addition, for 2-methylfuran deuteration of the methyl substituent was also observed to a large extent (50%). Because of the vastly different physicochemical and electronic properties of pyrroles, imidazoles, and furans, it is difficult to rationalize the regioselectivity for each substrate individually. In general, H/D exchange of hydrogen atoms ortho to a heteroatom is highly favorable and is most-likely directed by precoordination of the heteroatom to the metal center. Precoordination also explains the deuteration of the C(sp^3)−H bonds in 2-methyl furan (Table 1; [$\mathbf{d_3}$]-**18**). However, for 2,5-dimethylfuran ([$\mathbf{d_2}$]-**19**) and 2,6-dimethylpyridine ([$\mathbf{d_1}$]-**15**) coordination to the metal center is hampered due to steric crowding and deuteration of the C(sp^3)−H bonds is not observed. Furthermore, for 5-membered heterocycles, deuteration of C−H bonds adjacent

https://dx.doi.org/10.1021/jacs.0c07689
J. Am. Chem. Soc. 2020, 142, 17131−17139

to methyl substituents is more feasible because they are sterically more accessible compared to their 6-membered counterparts (e.g., compare [$\mathbf{d_2}$]-**16**−[$\mathbf{d_2}$]-**19** with [$\mathbf{d_1}$]-**15**). The exception appears to be *N*-methylpyrrole (Table 1, [**d2**]-**16**), whose lack of ortho reactivity we are not able to explain. For 6-membered aromatic heterocycles such as 2,6-lutidine deuteration was regioselective for the sterically most accessible para proton (Table 1, [$\mathbf{d_1}$]-**15**). For quinoline all aromatic C−H bonds were deuterated to yield quinoline-d_7 (Table 1, [$\mathbf{d_7}$]-**21**). The different degree of deuteration in quinolinereflects the different bond dissociation energies of the various C(sp^2)−H bonds.[33]

Comparing these results to the state-of-the-art, it was realized that despite the tremendous progress in homogeneous catalysis, earth-abundant metal catalyzed HIE at aromatic C(sp^2)-H bonds remains extremely rare.[27] For example, the cobalt catalyzed H/D exchange reported by Zou and co-workers is only applicable to indoles,[27b] while the cobalt catalysts developed by Chirik and co-workers primarily catalyze H/D exchange at (benzylic) C(sp^3)-H bonds.[27e] For iron related studies, the seminal work of Chirik and co-workers is important as it describes the first example of the iron catalyzed HIE at aromatic C(sp^2)-H bonds including those of pharmaceuticals.[27f] However, due to the instability of the in situ formed dihydride, hydrogen or deuterium gas is always required to ensure catalyst stability and efficiency as shown in a recent study.[27a] The herein reported results, however, demonstrate for the first time that such *trans*-dihydrides can be stable, ultimately leading to the deuteration of wide variety of aromatic hydrocarbons at lower temperatures with shorter reaction times and greater efficiencies,[27f] even when compared to PNP ruthenium dihydride complexes reported by Milstein and Leitner.[24a] However, it must be mentioned that comparison to the state-of-the-art is challenging due to the different nature of (i) the used solvents (e.g., benzene vs THF), (ii) the deuterium source (D_2, D_2O, or C_6D_6), and (iii) the used catalyst loadings.

Computational Mechanistic Investigations. To further understand the regioselectivity and to gain more insight into the mechanism of the H/D exchange between benzene-d_6 and (hetero)aromatic hydrocarbons, we used density functional theory (DFT) to obtain more detailed information about the relevant intermediates and transition states (Figures 3). To reduce the computational load, calculations were performed on a model system with R^1 = Me (Figure 3). Additional computational details are reported in the Supporting Information.

Before going into the details of the herein reported H/D exchange and C−H bond activation, there are several mechanisms by which C−H bonds can be activated that include (i) oxidative addition, (ii) σ-bond metathesis, and other types of mechanisms.[34] Low valent (late) transition metals generally activate C(sp^2)−H bonds via oxidative addition. High valent (early) transition metals, on the other hand, prefer a σ-bond metathesis pathway, because of their general lack of available d-electrons. A variant of σ-bond metathesis, σ-complex-assisted metathesis or σ-CAM, has also been developed for late transition metals in order to to explain the facile hydrogen exchange at bound E−H (E = B, C, or Si) σ -complexes.[35] For example, Leitner,[24a] Lau,[24b] and others,[36] have used σ-CAM to explain precious metal-catalyzed H/D exchange at aliphatic and aromatic hydrocarbons.

For iron, oxidative addition of C(sp^2)−H bonds is well-known and has been established for nearly half a century.[37] On the other hand, Eisenstein and co-workers have shown that, for iron, σ-CAM is another plausible mechanistic pathway for H/D exchange at aromatic hydrocarbons.[38] Our computational studies indeed indicate that H/D exchange with benzene-d_6 most likely occurs via a σ-CAM based mechanism (Figure 3). Starting from **3**, labeled **A** in Figure 3, formation of the σ-complex **C** is a two-step process and energetically uphill by 18.4 kcal mol^{-1}. The structure of intermediate C is shown in Figure 3 and features in an η^2_{C-H} interaction of benzene with the iron metal center resulting in elongation of the C−H bond by 0.032 Å. Such intermediates have also been implied for aromatic C(sp^2)−H activation with ruthenium and iridium.[39] The C(sp^2)-carbon atom engaged in the η^2_{C-H} interaction is located 0.125 Å above the plane of the $PC_{NHC}P$ pincer ligand, while the C_b-H_b bond is rotated upward by 27.0° and located 0.420 Å above the $PC_{NHC}P$ plane. The slight upward rotation, might indicate an attractive interaction between the axial deuteride (D1) and H_b as their calculated distance of 2.098 Å is slightly shorter than the sum of their van der Waals radii (2.200 Å).[38] The attractive interaction between D1 and the C_b-H_b bond is somewhat reminiscent of the hydride "cis effect" proposed by Eisenstein and Caulton,[40] which describes the interaction between a metal-hydride and a coordinated dihydrogen molecule en-route toward dynamic hydrogen atom exchange. As such the "cis-effect" demonstrates important concepts that are also observed in the herein described σ-CAM (vide infra).[35]

The critical C−H activation step occurs via a σ-complex-assisted metathesis pathway and leads to the formation of the nonclassical hydride isotopologue (**D**) with an overall energy barrier (ΔG) of 25.9 kcal mol^{-1}. The transition state structure (**TS1**) is shown in Figure 3 (bottom) and features an iron complex with a distorted pentagonal bipyramidal geometry. Obviously, starting from **C**, further distortion of the Fe···C axis is necessary to access the planar four-center transition state in **TS1** that is typically observed for σ-CAM based mechanisms. In **TS1**, the calculated D1···H_b and Fe···C_b distances of 1.193 and 2.106 Å are significantly shorter than those found by Leitner and Milstein,[24a] and are indicative of a σ-CAM based mechanism with a late transition-state structure exhibiting very little oxidative addition character as shown by Eisenstein and co-workers.[41] Overall, the barrier going from **C** to **D** is 7.5 kcal mol^{-1}, indicating that H/D exchange occurs quite readily once the σ-complex is formed and that the slightly elevated temperatures (50 °C) are necessary to facilitate dissociation of the N_2 ligand (Figure 3).

The formation of nonclassical hydride isotopologue **D** is also supported by NMR studies. Monitoring a solution of **2** in benzene-d_6 shows the formation of a triplet at −8.79 ppm ($^1J_{H-D}$ = 21.1 Hz) in the $^1H\{^{31}P\}$ NMR spectrum after 15 min (Figures S1−S4). The large value of the H−D coupling constant is indicative for the formation of a nonclassical hydride intermediate, as cis/trans HD couplings are general small or negligible.[42] In this process, oxidative addition from an Fe(0)/Fe(II) complex was not observed experimentally and computationally.

Rotation around the iron H−D bond (Figure 3, **D** → **E**) is essentially barrierless and the transition state structure **TS2** is shown in Figure 3 (bottom). The calculated bond lengths in **TS2** do not differ significantly from those calculated for **D** and the complex remains essentially octahedral. After rotation, the

https://dx.doi.org/10.1021/jacs.0c07689
J. Am. Chem. Soc. 2020, 142, 17131−17139

first stage of the H/D exchange is complete (Figure 3, **A** → **E**). Hereafter, a nearly identical, but reverse, pathway follows that start with σ-CAM to yield the σ-bonded deuterated benzene adduct (**F**). Final two-step ligand exchange between the substrate and N_2 regenerates an isotopologue of the starting catalyst (**H**). In general, the herein presented mechanism is similar to that proposed by Leitner and Milstein, whose ruthenium PNP complex also catalyzes H/D exchange between aromatic hydrocarbons and benzene-d_6.[24a] Besides the mechanism outlined in Figure 3, a modified version is also energetically accessible (Figure S76; path B). In this mechanism, instead from the *trans*-dideuteride, σ-CAM is initiated from the iron(II) *cis*-dideuteride with a very similar transition state that is only 5.2 kcal mol^{-1} higher in energy.

We also used computational studies to gain more insight into the observed regioselectivity. For a series of substituted benzenes, we calculated the energy barriers of **TS1-R** (Table 2; R = H, Me, NMe_2, OMe, and F). For benzene (R = H) the calculated barrier is 25.2 kcal mol^{-1} which is slightly lower than for TS1, due to isotope effects.[43] Overall, as our calculations will show, the observed regioselectivity is combination of steric and electronic effects. As expected strong steric effects are observed for toluene (R = Me; Table 2). The energy barrier for ortho C−H bond activation (30.4 kcal mol^{-1}) is significantly higher than for activation at the meta and para positions (ΔG = 25.9/25.2 kcal mol^{-1}). Similar effects are observed for dimethylaniline, where C−H bond activation at the ortho position has an energy barrier of 31.3 kcal mol^{-1} (Table 2). These results are in-line with our experimental results (Table 1)

Because for anisole no strong steric effects are expected and precoordination of the heteroatom is commonly invoked in C−H bond activation strategies, there are no clear differences in the energies for ortho, meta, or para C−H bond activation. As a result, complete deuteration of all C−H bonds is observed, including those present in the −OMe substituent (Tables 1 and 2).

Besides the obvious steric effects, electronic effects are also important. This is particularly evident in fluorinated substrates [$\mathbf{d_5}$]-**6** and [$\mathbf{d_2}$]-**9**. We begin by noting that the overall transition barriers **TS1-F** for C(sp^2)−H activation in fluorinated substrates are lower than those calculated for their nonfluorinated counterparts (Table 2). Despite having the strongest C−H bond, the more facile activation of fluoroarenes is well-known and is due to the larger increase of the M−C_{Ar} bond strength relative to that of the C_{Ar}−H bond.[44,45] This is particularly true when fluorine substituents are introduced at the ortho position as demonstrated by Jones and Perutz.[46] This pronounced *ortho*-fluorine effect is clearly seen in [$\mathbf{d_2}$]-**9**, which shown nearly exclusive deuteration (~85%) at ortho-position. Similarly, for fluorobenzene ([$\mathbf{d_5}$]-**6**), the highest level of deuteration is observed at ortho position (98%). In contrast, the para position shows a lower level of deuteration (~90%), consistent with a transition state barrier that is 1.2 kcal mol^{-1} higher than that calculated for the ortho position (Table 2). Besides the electronic of fluorine, other electronic effects are observed as well. To illustrate, we calculated the natural charges on the aromatic carbons and hydrogen atom H_b (Figure S79). As expected upon C−H bond activation, additional negative charges develop on aromatic carbon atoms (incl. C_b), while a positive charge develops on H_b. Consequently, π-donation of the coplanar NMe_2 substituent effectively destabilizes this negative charge, resulting in an overall higher activation energy for C−H bond activation (Table 2).

Overall, these computational studies show that for the majority of substrates the observed regioselectivity can be explained by a combination of steric and electronic factors (Table 2) and that a σ-CAM based mechanism is able to explain the observed HIE (Figure 3).

CONCLUSIONS

In summary, we have reported the synthesis and characterization of a rare *trans*-dihydride iron(II) dinitrogen complex (**2**) that is based on a novel $PC_{NHC}P$ pincer type motif. This compound is stable under N_2 for several days and can be used for selective H/D exchange at (hetero)aromatic hydrocarbons with benzene-d_6 as deuterium source. Deuterium incorporation typically exceeds 90% and is generally regioselective for sterically accessible C(sp^2)−H bonds unless overriding electronic effects are present. Computational studies indicate that a σ-bond metathesis pathway is probably responsible for the observed hydrogen isotope exchange (HIE), which is accessible under mild conditions (N_2, 50 °C). Overall, the herein reported results convey a convenient and straightforward method for H/D exchange that displays a wide functional group tolerance (e.g., esters, amides, halides, ethers, etc.). Furthermore, the robustness and stability of the herein reported catalyst holds great potential for other organic transformations that rely on hydride transfer or those that focus on small molecule activation. Current efforts are directed toward synthesizing the corresponding manganese, cobalt, and nickel complexes and exploring their reactivity in a variety of organic transformations.

ASSOCIATED CONTENT

Supporting Information

The Supporting Information is available free of charge at https://pubs.acs.org/doi/10.1021/jacs.0c07689.

Synthetic procedures, characterization data, catalysis, and computational studies (PDF)
xyz-coordinate files (ZIP)
Crystal data (CIF)

AUTHOR INFORMATION

Corresponding Author

Graham de Ruiter − *Schulich Faculty of Chemistry, Technion−Israel Institute of Technology, Technion City 3200008, Haifa, Israel;* orcid.org/0000-0001-6008-286X; Email: graham@technion.ac.il

Authors

Subhash Garhwal − *Schulich Faculty of Chemistry, Technion−Israel Institute of Technology, Technion City 3200008, Haifa, Israel;* orcid.org/0000-0002-0093-9224

Alexander Kaushansky − *Schulich Faculty of Chemistry, Technion−Israel Institute of Technology, Technion City 3200008, Haifa, Israel*

Natalia Fridman − *Schulich Faculty of Chemistry, Technion−Israel Institute of Technology, Technion City 3200008, Haifa, Israel*

Linda J. W. Shimon − *Department of Chemical Research Support, Weizmann Institute of Science, Rehovot 7610001, Israel;* orcid.org/0000-0002-7861-9247

Complete contact information is available at:

https://dx.doi.org/10.1021/jacs.0c07689
J. Am. Chem. Soc. 2020, 142, 17131−17139

https://pubs.acs.org/10.1021/jacs.0c07689

Notes

The authors declare no competing financial interest.

■ ACKNOWLEDGMENTS

Research was supported by the Azrieli Foundation (Israel), and the Technion EVPR Fund − Mallat Family Research Fund. G.d.R. is an Azrieli young faculty fellow and a Horev Fellow supported by the Taub Foundation. G.de.R. kindly acknowledges the Israel Science Foundation for a personal research Grant (574/20) and and equipment grant (579/20).

■ REFERENCES

(1) (a) Cornils, B.; Herrmann, W. A.; Beller, M.; Paciello, R. *Applied Homogeneous Catalysis with Organometallic Compounds: A Comprehensive Handbook in Four Vol.*, 3rd ed.; Wiley-VCH Verlag GmbH & Co: Weinheim, Germany, 2017. (b) Hartwig, J. F. *Organotransition Metal Chemistry: From Bonding to Catalysis*; University Science Books: Sausalito, CA, 2010.

(2) (a) Ludwig, J. R.; Schindler, C. S. Catalyst: Sustainable Catalysis. *Chem.* **2017**, *2*, 313−316. (b) Nakamura, E.; Sato, K. Managing the Scarcity of Chemical Elements. *Nat. Mater.* **2011**, *10*, 158−161.

(3) Hapke, M.; Hilt, G. *Cobalt Catalysis in Organic Synthesis: Methods and Reactions*; Wiley-VCH Verlag GmbH & Co: Weinheim, Germany, 2020.

(4) (a) Carney, J. R.; Dillon, B. R.; Thomas, S. P. Recent Advances of Manganese Catalysis for Organic Synthesis. *Eur. J. Org. Chem.* **2016**, *2016*, 3912−3929. (b) Liu, W.; Ackermann, L. Manganese-Catalyzed C-H Activation. *ACS Catal.* **2016**, *6*, 3743−3752.

(5) (a) Fürstner, A. Iron Catalysis in Organic Synthesis: A Critical Assessment of What It Takes To Make This Base Metal a Multitasking Champion. *ACS Cent. Sci.* **2016**, *2*, 778−789. (b) Bauer, I.; Knölker, H.-J. Iron Catalysis in Organic Synthesis. *Chem. Rev.* **2015**, *115*, 3170−3387.

(6) Gebbink, R. J. M. K.; Moret, M. E. *Non-Noble Metal Catalysis: Molecular Approaches and Reactions*; Wiley-VCH Verlag GmbH & Co: Weinheim, Germany, 2019.

(7) (a) Fritz, M.; Schneider, S. The Renaissance of Base Metal Catalysis Enabled by Functional Ligands. In *The Periodic Table II: Catalytic, Materials, Biological and Medical Applications*; Mingos, D. M. P., Ed.; Springer International Publishing: Cham, 2019; pp 1−36. (b) Holland, P. L. Reaction: Opportunities for Sustainable Catalysts. *Chem.* **2017**, *2*, 443−444.

(8) (a) Junge, K.; Papa, V.; Beller, M. Cobalt-Pincer Complexes in Catalysis. *Chem. - Eur. J.* **2019**, *25*, 122−143. (b) Alig, L.; Fritz, M.; Schneider, S. First-Row Transition Metal (De)Hydrogenation Catalysis Based On Functional Pincer Ligands. *Chem. Rev.* **2019**, *119*, 2681−2751. (c) Wen, H.; Liu, G.; Huang, Z. Recent Advances in Tridentate Iron and Cobalt Complexes gor Alkene and Alkyne Hydrofunctionalizations. *Coord. Chem. Rev.* **2019**, *386*, 138−153. (d) Mukherjee, A.; Milstein, D. Homogeneous Catalysis by Cobalt and Manganese Pincer Complexes. *ACS Catal.* **2018**, *8*, 11435−11469. (e) Gorgas, N.; Kirchner, K. Isoelectronic Manganese and Iron Hydrogenation/Dehydrogenation Catalysts: Similarities and Divergences. *Acc. Chem. Res.* **2018**, *51*, 1558−1569. (f) Bauer, G.; Hu, X. Recent Developments Of Iron Pincer Complexes For Catalytic Applications. *Inorg. Chem. Front.* **2016**, *3*, 741−765. (g) Farrell, K.; Albrecht, M. Late Transition Metal Complexes with Pincer Ligands that Comprise N-Heterocyclic Carbene Donor Sites. In *The Privileged Pincer-Metal Platform: Coordination Chemistry & Applications*; van Koten, G., Gossage, R. A., Eds.; Springer International Publishing: Cham, 2016; pp 45−91.

(9) (a) Jiang, Y.; Gendy, C.; Roesler, R. Nickel, Ruthenium, and Rhodium NCN-Pincer Complexes Featuring a Six-Membered N-Heterocyclic Carbene Central Moiety and Pyridyl Pendant Arms. *Organometallics* **2018**, *37*, 1123−1132. (b) Harris, C. F.; Bayless, M. B.; van Leest, N. P.; Bruch, Q. J.; Livesay, B. N.; Bacsa, J.; Hardcastle, K. I.; Shores, M. P.; de Bruin, B.; Soper, J. D. Redox-Active Bis(phenolate) N-Heterocyclic Carbene [OCO] Pincer Ligands Support Cobalt Electron Transfer Series Spanning Four Oxidation States. *Inorg. Chem.* **2017**, *56*, 12421−12435. (c) Brown, R. M.; Borau Garcia, J.; Valjus, J.; Roberts, C. J.; Tuononen, H. M.; Parvez, M.; Roesler, R. Ammonia Activation by a Nickel NCN-Pincer Complex featuring a Non-Innocent N-Heterocyclic Carbene: Ammine and Amido Complexes in Equilibrium. *Angew. Chem., Int. Ed.* **2015**, *54*, 6274−6277. (d) Kaplan, H. Z.; Li, B.; Byers, J. A. Synthesis and Characterization of a Bis(imino)-N-heterocyclic Carbene Analogue to Bis(imino)pyridine Iron Complexes. *Organometallics* **2012**, *31*, 7343−7350.

(10) (a) Subramaniyan, V.; Dutta, B.; Govindaraj, A.; Mani, G. Facile Synthesis of Pd(II) and Ni(II) Pincer Carbene Complexes by the Double C-H Bond Activation of a New Hexahydropyrimidine-Based Bis(Phosphine): Catalysis of C-N Couplings. *Dalton Trans.* **2019**, *48*, 7203−7210. (b) Sung, S.; Wang, Q.; Krämer, T.; Young, R. D. Synthesis and Reactivity of a PCcarbeneP Cobalt(I) Complex: The Missing Link in the Cobalt PXP Pincer Series (X = B, C, N). *Chem. Sci.* **2018**, *9*, 8234−8241. (c) Gutsulyak, D. V.; Piers, W. E.; Borau-Garcia, J.; Parvez, M. Activation of Water, Ammonia, and Other Small Molecules by PCcarbeneP Nickel Pincer Complexes. *J. Am. Chem. Soc.* **2013**, *135*, 11776−11779. (d) Steinke, T.; Shaw, B. K.; Jong, H.; Patrick, B. O.; Fryzuk, M. D.; Green, J. C. Noninnocent Behavior of Ancillary Ligands: Apparent Trans Coupling of a Saturated N-Heterocyclic Carbene Unit with an Ethyl Ligand Mediated by Nickel. *J. Am. Chem. Soc.* **2009**, *131*, 10461−10466.

(11) Dröge, T.; Glorius, F. The Measure of All Rings—N-Heterocyclic Carbenes. *Angew. Chem., Int. Ed.* **2010**, *49*, 6940−6952.

(12) (a) Eizawa, A.; Arashiba, K.; Tanaka, H.; Kuriyama, S.; Matsuo, Y.; Nakajima, K.; Yoshizawa, K.; Nishibayashi, Y. Remarkable Catalytic Activity of Dinitrogen-Bridged Dimolybdenum Complexes Bearing NHC-Based PCP-Pincer Ligands Toward Nitrogen Fixation. *Nat. Commun.* **2017**, *8*, 14874. (b) Plikhta, A.; Pöthig, A.; Herdtweck, E.; Rieger, B. Toward New Organometallic Architectures: Synthesis of Carbene-Centered Rhodium and Palladium Bisphosphine Complexes. Stability and Reactivity of [PCBImPRh(L)][PF_6] Pincers. *Inorg. Chem.* **2015**, *54*, 9517−9528.

(13) Baker, T. M.; Mako, T. L.; Vasilopoulos, A.; Li, B.; Byers, J. A.; Neidig, M. L. Magnetic Circular Dichroism and Density Functional Theory Studies of Iron(II)-Pincer Complexes: Insight into Electronic Structure and Bonding Effects of Pincer N-Heterocyclic Carbene Moieties. *Organometallics* **2016**, *35*, 3692−3700.

(14) For earth-abundant metal catalysis with other types of carbene pincer complexes see: (a) Harris, C. F.; Kuehner, C. S.; Bacsa, J.; Soper, J. D. Photoinduced Cobalt(III)-Trifluoromethyl Bond Activation Enables Arene C-H Trifluoromethylation. *Angew. Chem., Int. Ed.* **2018**, *57*, 1311−1315. (b) Manna, C. M.; Kaplan, H. Z.; Li, B.; Byers, J. A. High Molecular Weight Poly(Lactic Acid) Produced by an Efficient Iron Catalyst Bearing a Bis(Amidinato)-N-Heterocyclic Carbene Ligand. *Polyhedron* **2014**, *84*, 160−167.

(15) (a) Morris, R. H. Mechanisms of the H_2- and Transfer Hydrogenation of Polar Bonds Catalyzed by Iron Group Hydrides. *Dalton Trans.* **2018**, *47*, 10809−10826. (b) Yu, R. P.; Darmon, J. M.; Semproni, S. P.; Turner, Z. R.; Chirik, P. J. Synthesis of Iron Hydride Complexes Relevant to Hydrogen Isotope Exchange in Pharmaceuticals. *Organometallics* **2017**, *36*, 4341−4343. (c) Gorgas, N.; Alves, L. G.; Stöger, B.; Martins, A. M.; Veiros, L. F.; Kirchner, K. Stable, Yet Highly Reactive Nonclassical Iron(II) Polyhydride Pincer Complexes: Z-Selective Dimerization and Hydroboration of Terminal Alkynes. *J. Am. Chem. Soc.* **2017**, *139*, 8130−8133. (d) Gorgas, N.; Stöger, B.; Veiros, L. F.; Kirchner, K. Highly Efficient and Selective Hydrogenation of Aldehydes: A Well-Defined Fe(II) Catalyst Exhibits Noble-Metal Activity. *ACS Catal.* **2016**, *6*, 2664−2672. (e) Langer, R.; Diskin-Posner, Y.; Leitus, G.; Shimon, L. J. W.; Ben-David, Y.; Milstein, D. Low-Pressure Hydrogenation of Carbon Dioxide Catalyzed by an Iron Pincer Complex Exhibiting Noble Metal Activity. *Angew. Chem., Int. Ed.* **2011**, *50*, 9948−9952. (f) Langer, R.;

Leitus, G.; Ben-David, Y.; Milstein, D. Efficient Hydrogenation of Ketones Catalyzed by an Iron Pincer Complex. *Angew. Chem., Int. Ed.* **2011**, *50*, 2120−2124. (g) Yu, Y.; Sadique, A. R.; Smith, J. M.; Dugan, T. R.; Cowley, R. E.; Brennessel, W. W.; Flaschenriem, C. J.; Bill, E.; Cundari, T. R.; Holland, P. L. The Reactivity Patterns of Low-Coordinate Iron-Hydride Complexes. *J. Am. Chem. Soc.* **2008**, *130*, 6624−6638.

(16) Trovitch, R. J.; Lobkovsky, E.; Chirik, P. J. Bis(diisopropylphosphino)pyridine Iron Dicarbonyl, Dihydride, and Silyl Hydride Complexes. *Inorg. Chem.* **2006**, *45*, 7252−7260.

(17) (a) Fuku-En, S.-i.; Yamamoto, J.; Kojima, S.; Yamamoto, Y. Synthesis and Application of New Dipyrido-Annulated N-heterocyclic Carbene with Phosphorus Substituents. *Chem. Lett.* **2014**, *43*, 468−470. (b) Fuku-En, S.-i.; Yamamoto, J.; Minoura, M.; Kojima, S.; Yamamoto, Y. Synthesis of New Dipyrido-Annulated N-Heterocyclic Carbenes with Ortho Substituents. *Inorg. Chem.* **2013**, *52*, 11700−11702. (c) Gierz, V.; Seyboldt, A.; Maichle-Moessmer, C.; Froehlich, R.; Rominger, F.; Kunz, D. Straightforward Synthesis of Dipyrido-Annelated NHC-palladium(II) Complexes by Oxidative Addition. *Eur. J. Inorg. Chem.* **2012**, *2012*, 1423−1429. (d) Nonnenmacher, M.; Kunz, D.; Rominger, F. Synthesis and Catalytic Properties Of Rhodium(I) and Copper(I) Complexes Bearing Dipyrido-Annulated N-Heterocyclic Carbene Ligands. *Organometallics* **2008**, *27*, 1561−1568. (e) Nonnenmacher, M.; Kunz, D.; Rominger, F.; Oeser, T. X-Ray Crystal Structures of 10π- and 14π-Electron Pyrido-Annelated N-Heterocyclic Carbenes. *Chem. Commun.* **2006**, 1378−1380. (f) Nonnenmacher, M.; Kunz, D.; Rominger, F.; Oeser, T. First Examples of Dipyrido[1,2-C:2′,1′-E]Imidazolin-7-Ylidenes Serving as NHC-Ligands: Synthesis, Properties and Structural Features of their Chromium and Tungsten Pentacarbonyl Complexes. *J. Organomet. Chem.* **2005**, *690*, 5647−5653.

(18) (a) Schremmer, C.; Cordes, C.; Klawitter, I.; Bergner, M.; Schiewer, C. E.; Dechert, S.; Demeshko, S.; John, M.; Meyer, F. Spin-State Variations of Iron(III) Complexes with Tetracarbene Macrocycles. *Chem. - Eur. J.* **2019**, *25*, 3918−3929. (b) Schneider, H.; Schmidt, D.; Eichhöfer, A.; Radius, M.; Weigend, F.; Radius, U. Synthesis and Reactivity of NHC-Stabilized Iron(II)-Mesityl Complexes. *Eur. J. Inorg. Chem.* **2017**, *2017*, 2600−2616. (c) Liang, Q.; Janes, T.; Gjergji, X.; Song, D. Iron Complexes of a Bidentate Picolyl-NHC Ligand: Synthesis, Structure and Reactivity. *Dalton Trans.* **2016**, *45*, 13872−13880. (d) Ouyang, Z.; Du, J.; Wang, L.; Kneebone, J. L.; Neidig, M. L.; Deng, L. Linear and T-Shaped Iron(I) Complexes Supported by N-Heterocyclic Carbene Ligands: Synthesis and Structure Characterization. *Inorg. Chem.* **2015**, *54*, 8808−8816. (e) Zlatogorsky, S.; Muryn, C. A.; Tuna, F.; Evans, D. J.; Ingleson, M. J. Synthesis, Structures, and Reactivity of Chelating Bis-N-Heterocyclic-Carbene Complexes of Iron(II). *Organometallics* **2011**, *30*, 4974−4982.

(19) (a) Wiedner, E. S.; Chambers, M. B.; Pitman, C. L.; Bullock, R. M.; Miller, A. J. M.; Appel, A. M. Thermodynamic Hydricity of Transition Metal Hydrides. *Chem. Rev.* **2016**, *116*, 8655−8692. (b) Wang, D.; Astruc, D. The Golden Age of Transfer Hydrogenation. *Chem. Rev.* **2015**, *115*, 6621−6686. (c) Larionov, E.; Li, H.; Mazet, C. Well-Defined Transition Metal Hydrides in Catalytic Isomerizations. *Chem. Commun.* **2014**, *50*, 9816−9826. (d) Pospech, J.; Fleischer, I.; Franke, R.; Buchholz, S.; Beller, M. Alternative Metals for Homogeneous Catalyzed Hydroformylation Reactions. *Angew. Chem., Int. Ed.* **2013**, *52*, 2852−2872. (e) *Recent Advances in Hydride Chemistry*; Peruzzini, M., Poli, R., Eds.; Elsevier: Amsterdam, 2001; pp 1−578.

(20) *trans*-Dihydride iron complexes lacking stabilizing carbonyl ligands, readily reductively eliminate H_2 when exposed to an atmosphere N_2. The resulting Fe(0) complexes are either (I) inactive for HIE, see for example: Yu, R. P.; Darmon, J. M.; Semproni, S. P.; Turner, Z. R.; Chirik, P. J. Synthesis of Iron Hydride Complexes Relevant to Hydrogen Isotope Exchange in Pharmaceuticals. *Organometallics* **2017**, *36*, 4341−4343. or (ii) they are very sluggish catalysts for HIE exchange see: Corpas, J.; Viereck, P.; Chirik, P. J. C(sp^2)-H Activation with Pyridine Dicarbene Iron Dialkyl Complexes: Hydrogen Isotope Exchange of Arenes Using Benzene-d_6 as a Deuterium Source. *ACS Catal.* **2020**, *10*, 8640−8647.

(21) (a) Parkin, G. Applications of Deuterium Isotope Effects for Probing Aspects of Reactions Involving Oxidative Addition and Reductive Elimination of H-H and C-H Bonds. *J. Labelled Compd. Radiopharm.* **2007**, *50*, 1088−1114. (b) Jones, W. D. Isotope Effects in C-H Bond Activation Reactions by Transition Metals. *Acc. Chem. Res.* **2003**, *36*, 140−146.

(22) (a) Katsnelson, A. Heavy Drugs Draw Heavy Interest From Pharma Backers. *Nat. Med.* **2013**, *19*, 656−656. (b) Elmore, C. S. The Use of Isotopically Labeled Compounds in Drug Discovery. In *Annu. Rep. Med. Chem.*; Macor, J. E., Ed.; Academic Press: New York, 2009; Vol. *44*, pp 515−534.

(23) Atzrodt, J.; Derdau, V.; Kerr, W. J.; Reid, M. Deuterium- and Tritium-Labelled Compounds: Applications in the Life Sciences. *Angew. Chem., Int. Ed.* **2018**, *57*, 1758−1784.

(24) (a) Prechtl, M. H. G.; Hölscher, M.; Ben-David, Y.; Theyssen, N.; Loschen, R.; Milstein, D.; Leitner, W. H/D Exchange at Aromatic and Heteroaromatic Hydrocarbons Using D_2O as the Deuterium Source and Ruthenium Dihydrogen Complexes as the Catalyst. *Angew. Chem., Int. Ed.* **2007**, *46*, 2269−2272. (b) Ng, S. M.; Lam, W. H.; Mak, C. C.; Tsang, C. W.; Jia, G.; Lin, Z.; Lau, C. P. C-H Bond Activation by a Hydrotris(pyrazolyl)borato Ruthenium Hydride Complex. *Organometallics* **2003**, *22*, 641−651.

(25) (a) Di Giuseppe, A.; Castarlenas, R.; Pérez-Torrente, J. J.; Lahoz, F. J.; Oro, L. A. Hydride-Rhodium(III)-N-Heterocyclic Carbene Catalysts for Vinyl-Selective H/D Exchange: A Structure-Activity Study. *Chem. - Eur. J.* **2014**, *20*, 8391−8403. (b) Lenges, C. P.; White, P. S.; Brookhart, M. Hydrogen/Deuterium Exchange Reactions and Transfer Hydrogenations Catalyzed by [C_5Me_5Rh-(olefin)$_2$] Complexes: Conversion of Alkoxysilanes to Silyl Enolates. *J. Am. Chem. Soc.* **1999**, *121*, 4385−4396. (c) Blake, M. R.; Garnett, J. L.; Gregor, I. K.; Hannan, W.; Hoa, K.; Long, M. A. Rhodium Trichloride as a Homogeneous Catalyst for Isotopic Hydrogen Exchange. Comparison with Heterogeneous Rhodium in the Deuteriation of Aromatic Compounds and Alkanes. *J. Chem. Soc., Chem. Commun.* **1975**, 930−932.

(26) (a) Nilsson, G. N.; Kerr, W. J. The Development and use of Novel Iridium Complexes as Catalysts for Ortho-Directed Hydrogen Isotope Exchange Reactions. *J. Labelled Compd. Radiopharm.* **2010**, *53*, 662−667. (b) Corberán, R.; Sanaú, M.; Peris, E. Highly Stable Cp*-Ir(III) Complexes with N-Heterocyclic Carbene Ligands as C-H Activation Catalysts for the Deuteration of Organic Molecules. *J. Am. Chem. Soc.* **2006**, *128*, 3974−3979. (c) Yung, C. M.; Skaddan, M. B.; Bergman, R. G. Stoichiometric and Catalytic H/D Incorporation by Cationic Iridium Complexes: A Common Monohydrido-Iridium Intermediate. *J. Am. Chem. Soc.* **2004**, *126*, 13033−13043. (d) Klei, S. R.; Golden, J. T.; Tilley, T. D.; Bergman, R. G. Iridium-Catalyzed H/D Exchange into Organic Compounds in Water. *J. Am. Chem. Soc.* **2002**, *124*, 2092−2093. (e) Ellames, G. J.; Gibson, J. S.; Herbert, J. M.; McNeill, A. H. The Scope and Limitations of Deuteration Mediated by Crabtree's Catalyst. *Tetrahedron* **2001**, *57*, 9487−9497. (f) Heys, R. Investigation of [$IrH_2(Me_2CO)_2(PPh_3)_2$]BF_4 as a Catalyst of Hydrogen Isotope Exchange of Substrates in Solution. *J. Chem. Soc., Chem. Commun.* **1992**, 680−681.

(27) (a) Corpas, J.; Viereck, P.; Chirik, P. J. C(sp^2)-H Activation with Pyridine Dicarbene Iron Dialkyl Complexes: Hydrogen Isotope Exchange of Arenes Using Benzene-d_6 as a Deuterium Source. *ACS Catal.* **2020**, *10*, 8640−8647. (b) Zhang, J.; Zhang, S.; Gogula, T.; Zou, H. Versatile Regioselective Deuteration of Indoles via Transition-Metal-Catalyzed H/D Exchange. *ACS Catal.* **2020**, *10*, 7486−7494. (c) Zarate, C.; Yang, H.; Bezdek, M. J.; Hesk, D.; Chirik, P. J. Ni(I)-X Complexes Bearing a Bulky α-Diimine Ligand: Synthesis, Structure, and Superior Catalytic Performance in the Hydrogen Isotope Exchange in Pharmaceuticals. *J. Am. Chem. Soc.* **2019**, *141*, 5034−5044. (d) Yang, H.; Zarate, C.; Palmer, W. N.; Rivera, N.; Hesk, D.; Chirik, P. J. Site-Selective Nickel-Catalyzed Hydrogen Isotope Exchange in N-Heterocycles and Its Application to the Tritiation of Pharmaceuticals. *ACS Catal.* **2018**, *8*, 10210−10218.

https://dx.doi.org/10.1021/jacs.0c07689
J. Am. Chem. Soc. 2020, 142, 17131−17139

(e) Palmer, W. N.; Chirik, P. J. Cobalt-Catalyzed Stereoretentive Hydrogen Isotope Exchange of C(sp^3)-H Bonds. *ACS Catal.* **2017**, *7*, 5674−5678. (f) Pony Yu, R.; Hesk, D.; Rivera, N.; Pelczer, I.; Chirik, P. J. Iron-Catalysed Tritiation of Pharmaceuticals. *Nature* **2016**, *529*, 195−199. (g) Lenges, C. P.; White, P. S.; Marshall, W. J.; Brookhart, M. Synthesis, Structure, and Reactivity of [C_5Me_5CoLL'] Complexes with L = Pyridine and L' = Olefin or L-L' = Bipyridine. *Organometallics* **2000**, *19*, 1247−1254.

(28) (a) Yang, H.; Hesk, D. Base Metal-Catalyzed Hydrogen Isotope Exchange. *J. Labelled Compd. Radiopharm.* **2020**, *63*, 296−307. (b) Atzrodt, J.; Derdau, V.; Fey, T.; Zimmermann, J. The Renaissance of H/D Exchange. *Angew. Chem., Int. Ed.* **2007**, *46*, 7744−7765.

(29) (a) Zhou, J.; Hartwig, J. F. Iridium-Catalyzed H/D Exchange at Vinyl Groups without Olefin Isomerization. *Angew. Chem., Int. Ed.* **2008**, *47*, 5783−5787. (b) Feng, Y.; Lail, M.; Foley, N. A.; Gunnoe, T. B.; Barakat, K. A.; Cundari, T. R.; Petersen, J. L. Hydrogen-Deuterium Exchange between TpRu(PMe_3)(L)X (L = PMe_3 and X = OH, OPh, Me, Ph, or NHPh; L = NCMe and X = Ph) and Deuterated Arene Solvents: Evidence for Metal-Mediated Processes. *J. Am. Chem. Soc.* **2006**, *128*, 7982−7994. (c) Giunta, D.; Hölscher, M.; Lehmann, C. W.; Mynott, R.; Wirtz, C.; Leitner, W. Room Temperature Activation of Aromatic C-H Bonds by Non-Classical Ruthenium Hydride Complexes Containing Carbene Ligands. *Adv. Synth. Catal.* **2003**, *345*, 1139−1145. (d) Golden, J. T.; Andersen, R. A.; Bergman, R. G. Exceptionally Low-Temperature Carbon-Hydrogen/Carbon-Deuterium Exchange Reactions of Organic and Organometallic Compounds Catalyzed by the Cp*(PMe_3)IrH($ClCH_2Cl$)$^+$ Cation. *J. Am. Chem. Soc.* **2001**, *123*, 5837−5838.

(30) (a) Smith, S. A. M.; Lagaditis, P. O.; Lüpke, A.; Lough, A. J.; Morris, R. H. Unsymmetrical Iron P-NH-P' Catalysts for the Asymmetric Pressure Hydrogenation of Aryl Ketones. *Chem. - Eur. J.* **2017**, *23*, 7212−7216. (b) Sonnenberg, J. F.; Wan, K. Y.; Sues, P. E.; Morris, R. H. Ketone Asymmetric Hydrogenation Catalyzed by P-NH-P' Pincer Iron Catalysts: An Experimental and Computational Study. *ACS Catal.* **2017**, *7*, 316−326. (c) Yang, X. Unexpected Direct Reduction Mechanism for Hydrogenation of Ketones Catalyzed by Iron PNP Pincer Complexes. *Inorg. Chem.* **2011**, *50*, 12836−12843.

(31) Morello, G. R.; Hopmann, K. H. A Dihydride Mechanism Can Explain the Intriguing Substrate Selectivity of Iron-PNP-Mediated Hydrogenation. *ACS Catal.* **2017**, *7*, 5847−5855.

(32) After addition of the ketone, the reaction mixture turns from yellow/brown to dark green, which might indicate formation of an iron(0) species. Other iron(0) species have been isolated by us, which are all green. However, formation of a metal-enolate species, or stoichiometric reduction of the ketone cannot be exclusively excluded.

(33) (a) Wren, S. W.; Vogelhuber, K. M.; Garver, J. M.; Kato, S.; Sheps, L.; Bierbaum, V. M.; Lineberger, W. C. C-H Bond Strengths and Acidities in Aromatic Systems: Effects of Nitrogen Incorporation in Mono-, Di-, and Triazines. *J. Am. Chem. Soc.* **2012**, *134*, 6584−6595. (b) Luo, Y. R. *Handbook of Bond Dissociation Energies in Organic Compounds*; CRC Press: Boca Raton, FL, 2002.

(34) (a) Gandeepan, P.; Müller, T.; Zell, D.; Cera, G.; Warratz, S.; Ackermann, L. 3d Transition Metals for C-H Activation. *Chem. Rev.* **2019**, *119*, 2192−2452. (b) Balcells, D.; Clot, E.; Eisenstein, O. C—H Bond Activation in Transition Metal Species from a Computational Perspective. *Chem. Rev.* **2010**, *110*, 749−823. (c) Labinger, J. A.; Bercaw, J. E. Understanding and Exploiting C-H Bond Activation. *Nature* **2002**, *417*, 507−514. (d) Shilov, A. E.; Shul'pin, G. B. Activation of C-H Bonds by Metal Complexes. *Chem. Rev.* **1997**, *97*, 2879−2932.

(35) Perutz, R. N.; Sabo-Etienne, S. The σ-CAM Mechanism: σ Complexes as the Basis of σ-Bond Metathesis at Late-Transition-Metal Centers. *Angew. Chem., Int. Ed.* **2007**, *46*, 2578−2592.

(36) Di Giuseppe, A.; Castarlenas, R.; Oro, L. A. Mechanistic Considerations on Catalytic H/D Exchange Mediated by Organometallic Transition Tetal Complexes. *C. R. Chim.* **2015**, *18*, 713−741.

(37) (a) Dombray, T.; Werncke, C. G.; Jiang, S.; Grellier, M.; Vendier, L.; Bontemps, S.; Sortais, J.-B.; Sabo-Etienne, S.; Darcel, C. Iron-Catalyzed C-H Borylation of Arenes. *J. Am. Chem. Soc.* **2015**, *137*, 4062−4065. (b) Azizian, H.; Morris, R. H. Photochemical Synthesis and Reactions of FeH($C_6H_4PPhCH_2CH_2PPh_2$)-($PPh_2PCH_2CH2PPh_2$). *Inorg. Chem.* **1983**, *22*, 6−9. (c) Tolman, C. A.; Ittel, S. D.; English, A. D.; Jesson, J. P. Chemistry of 2-Naphthyl Bis[bis(dimethylphosphino)ethane] Hydride Complexes of Iron, Ruthenium, and Osmium. 3. Cleavage of sp^2 Carbon-Hydrogen Bonds. *J. Am. Chem. Soc.* **1979**, *101*, 1742−1751. (d) Hata, G.; Kondo, H.; Miyake, A. Ethylenebis(Diphenylphosphine) Complexes of Iron And Cobalt. Hydrogen Transfer between the Ligand and Iron Atom. *J. Am. Chem. Soc.* **1968**, *90*, 2278−2281.

(38) Mantina, M.; Chamberlin, A. C.; Valero, R.; Cramer, C. J.; Truhlar, D. G. Consistent van der Waals Radii for the Whole Main Group. *J. Phys. Chem. A* **2009**, *113*, 5806−5812.

(39) Ben-Ari, E.; Cohen, R.; Gandelman, M.; Shimon, L. J. W.; Martin, J. M. L.; Milstein, D. Ortho C-H Activation of Haloarenes and Anisole by an Electron-Rich Iridium(I) Complex: Mechanism and Origin of Regio- and Chemoselectivity. AnExperimental and TheoreticalStudy. *Organometallics* **2006**, *25*, 3190−3210.

(40) Van der Sluys, L. S.; Eckert, J.; Eisenstein, O.; Hall, J. H.; Huffman, J. C.; Jackson, S. A.; Koetzle, T. F.; Kubas, G. J.; Vergamini, P. J.; Caulton, K. G. An Attractive *cis*-Effect of Hydride on Neighbor Ligands: Experimental and Theoretical Studies on the Structure and Intramolecular Rearrangements of Fe(H)$_2$(η^2-H_2)($PEtPh_2$)$_3$. *J. Am. Chem. Soc.* **1990**, *112*, 4831−4841.

(41) Lam, W. H.; Jia, G.; Lin, Z.; Lau, C. P.; Eisenstein, O. Theoretical Studies on the Metathesis Processes, [Tp(PH_3)MR(η^2-H-CH_3)]-[Tp(PH_3)M(CH_3)(η^2-H-R)] (M = Fe, Ru, and Os; R = H and CH_3). *Chem. - Eur. J.* **2003**, *9*, 2775−2782.

(42) (a) Crabtree, R. H. Dihydrogen Complexation. *Chem. Rev.* **2016**, *116*, 8750−8769. (b) Morris, R. H. Dihydrogen, Dihydride and in Between: NMR and Structural Properties of Iron Group Complexes. *Coord. Chem. Rev.* **2008**, *252*, 2381−2394. (c) Jessop, P. G.; Morris, R. H. Reactions of Transition Metal Dihydrogen Complexes. *Coord. Chem. Rev.* **1992**, *121*, 155−284.

(43) Computationally, the only difference between hydrogen and deuterium atoms are in the vibrational modes, as a result the respective potential energy surfaces (PESs) will be nearly identical except for their relative energies. Typically, PESs that include deuterium are slightly higher in energy (*ca.* 0.4 kcal/mol). For more information see the Supporting Information for additional computational details.

(44) (a) Clot, E.; Mégret, C.; Eisenstein, O.; Perutz, R. N. Exceptional Sensitivity of Metal-Aryl Bond Energies to *ortho*-Fluorine Substituents: Influence of the Metal, the Coordination Sphere, and the Spectator Ligands on M-C/H-C Bond Energy Correlations. *J. Am. Chem. Soc.* **2009**, *131*, 7817−7827. (b) Evans, M. E.; Burke, C. L.; Yaibuathes, S.; Clot, E.; Eisenstein, O.; Jones, W. D. Energetics of C-H Bond Activation of Fluorinated Aromatic Hydrocarbons Using a [Tp'Rh(CNneopentyl)] Complex. *J. Am. Chem. Soc.* **2009**, *131*, 13464−13473. (c) Clot, E.; Besora, M.; Maseras, F.; Mégret, C.; Eisenstein, O.; Oelckers, B.; Perutz, R. N. Bond Energy M-C/H-C Correlations: Dual Theoretical and Experimental Approach to the Sensitivity of M-C Bond Strength to Substituents. *Chem. Commun.* **2003**, 490−491.

(45) For M-C/H-C bond energy correlations in nonfluorinated systems see: (a) Clot, E.; Mégret, C.; Eisenstein, O.; Perutz, R. N. Validation of the M-C/H-C Bond Enthalpy Relationship through Application of Density Functional Theory. *J. Am. Chem. Soc.* **2006**, *128*, 8350−8357. (b) Jones, W. D.; Hessell, E. T. Photolysis of Tp'Rh(Cn-Neopentyl)(η^2-PhN:C:N-Neopentyl) in Alkanes and Arenes: Kinetic and Thermodynamic Selectivity ff [Tp'Rh(Cn-Neopentyl)] for Various Types of Carbon-Hydrogen Bonds. *J. Am. Chem. Soc.* **1993**, *115*, 554−562.

(46) Selmeczy, A. D.; Jones, W. D.; Partridge, M. G.; Perutz, R. N. Selectivity in the Activation of Fluorinated Aromatic Hydrocarbons by Rhodium Complexes [(C_5H_5)Rh(PMe_3)] and [(C_5Me_5)Rh(PMe_3)]. *Organometallics* **1994**, *13*, 522−532.

https://dx.doi.org/10.1021/jacs.0c07689
J. Am. Chem. Soc. 2020, 142, 17131−17139